International Journal of Biological Macromolecules 149 (2020) 844–852

Contents lists available at ScienceDirect

International Journal of Biological Macromolecules

journal homepage: http://www.elsevier.com/locate/ijbiomac

Chitosan-mediated synthesis of biogenic silver nanoparticles (AgNPs), nanoparticle characterisation and *in vitro* assessment of anticancer activity in human hepatocellular carcinoma HepG2 cells

Kannappan Priya [a,*,1], Mayakrishnan Vijayakumar [b,*,1], Balakarthikeyan Janani [a]

[a] Department of Biochemistry, PSG College of Arts and Science (Autonomous), Affiliated to Bharathiar University, Coimbatore 641014, Tamil Nadu, India
[b] Department of Nutrition, Dairy Science Division, National Institute of Animal Science, Rural Development Administration, Cheonan-si, Chungcheongnam-do 31000, Republic of Korea

ARTICLE INFO

Article history:
Received 17 January 2020
Received in revised form 28 January 2020
Accepted 2 February 2020
Available online 3 February 2020

Keywords:
Chitosan
Nanoparticle
TEM
Cytotoxicity
Apoptosis

ABSTRACT

The biopolymer chitosan is currently in widespread use because of its nontoxicity, biocompatibility and biodegradability. Therefore, in this study, chitosan extracted from shrimp shells was used to synthesise biogenic silver nanoparticles (AgNPs). UV–visible spectrophotometry of reduced silver nanoparticles in the colloidal solution showed a single peak at 400 nm, confirming the formation of AgNPs. The presence of biomolecules responsible for reducing and capping the biogenic AgNPs was confirmed by FTIR. Surface morphology of the biosynthesised AgNPs was characterised using SEM, and TEM analysis showed the formation of spherical shapes 17–50 nm. The presence of elemental silver in the synthesised biogenic AgNPs was confirmed using EDX and the crystalline structure characterised by XRD. Cytotoxicity of biogenic AgNPs was determined using MTT and the trypan blue exclusion assay. Morphological changes in HepG2 cells were detected by analysis of the DNA ladder pattern *via* gel electrophoresis, and the IC_{50} of HepG2 cell inhibition by AgNPs was 48 μg/ml. The upregulated caspase 3 and 9 protein expression results confirmed cell death *via* apoptosis. In conclusion, chitosan has the ability to synthesise AgNPs with *in vitro* apoptotic activities.

© 2020 Published by Elsevier B.V.

1. Introduction

Nanoscience is the study of the design, synthesis and manipulation of nano-size (1–100 nm) materials [1]. Nanoparticles have unique electronic, optical and chemical properties, which differ from those observed in the bulk molecules [2]. Nanotechnology is a promising and rapidly growing area in science and technology with a wide range of applications in the biotechnology, textile, cosmetic and biomedical industries. In recent years, nanoparticles have demonstrated great potential in biomedical applications, particularly in biosensors, drug delivery, diagnostic tools and cancer treatment [3,4].

Nanomaterials are often made of gold, copper, magnesium, zinc or silver, the last of which has demonstrated good antibacterial, antifungal and antiviral activity [5,6]. Silver nanoparticles (AgNPs) can be used as coatings, intercalation material in electrical batteries, catalysts in chemical reactions, optical receptors and biological labelling. Researchers believe that the high antimicrobial activity of AgNPs is due to their large surface area, which directly interacts with microorganisms [7].

Nanoparticles can be synthesised by many methods including chemical, electrochemical and photochemical reduction. Unfortunately, conventional chemical and physical methods are generally expensive and generate toxic by-products which cause environmental hazards and health-related issues. To overcome these issues, a biological method has been developed which is free of toxic chemicals and requires less energy, so it is safer for the environment [8]. This promising alternative method employs bacteria, fungi, algae, viruses, plants and their by-products, such as polysaccharides, biopolymers, vitamins, proteins, lipids and plant extracts [9,10]. Polymeric nano-composites with silver nanoparticles are particularly good building blocks for medicinal and optoelectronic products because of the distinctive characteristics of nano-sized silver, as well as poly-functional nature of the polymer matrix [11,12]. The aim of this study was to apply the polysaccharide chitosan for silver nanoparticle synthesis and to optimise the synthesis of AgNPs using chitosan extracted from shrimp shell waste. In addition, the *in vitro* anticancer potential of AgNPs against human hepatocellular carcinoma HepG2 cells was investigated.

* Corresponding authors.
E-mail addresses: priyak08@gmail.com (K. Priya), marulbiochem@rediffmail.com (M. Vijayakumar).
[1] These authors contributed equally to this work.

https://doi.org/10.1016/j.ijbiomac.2020.02.007
0141-8130/© 2020 Published by Elsevier B.V.

2. Materials and methods

2.1. Collection and processing of shrimp shell waste

The shrimp wastes were collected from the local fish market in Coimbatore, India. The shells were removed, scraped clean of flesh, washed with copious water, dried and stored at −20 °C in an airtight container until further process.

2.2. Preparation of chitosan

For demineralisation, the shrimp shells were weighed (100 g) and transferred to a beaker containing 1.25 N HCl (volume 1:4, shell to HCl) and the mixture incubated for 3 h; this step was repeated 3–4 times. Following demineralisation, the shrimp shells were incubated in 5% (w/w) NaOH (volume 1:5, shell to NaOH), and this mixture heated for 1 h at 70–75 °C in a water bath to eradicate the protein. This deproteinisation process was repeated numerous times. The shells were heated to 60–65 °C, then crushed and the powder obtained was stored as chitin. To prepare chitosan, the chitin was deacetylated in 40% NaOH (volume 1:5, chitin to NaOH) and heated at 100 °C for 5–6 h. The NaOH was drained, the product rinsed with water several times, dried in the oven at 65 °C for 8 h and finally, the collected chitosan powder was stored for further use [13].

2.3. Synthesis of biogenic AgNPs

Biogenic AgNPs using chitosan were produced by methods published previously [14]. Briefly, 1% (w/v) of chitosan was dissolved in 150 ml of 0.5 M acetic acid and stirred for 12 h to obtain a clear solution. Freshly-prepared $AgNO_3$ (60 ml of 100 mM) was mixed with the acetic acid-chitosan solution. The solution was mixed by stirring for 12 h at 95 °C. After the solution colour changed, it was centrifuged at 6000 rpm for 10 min. The supernatant was removed and the pellet dried at 70 °C in an oven for 24 h. Finally, the obtained biogenic AgNPs powder was freeze-dried and the suspension was stored using Fisher Bioblock Scientific ultrasonic cleaning container.

2.4. Characterisation of AgNPs

2.4.1. UV–visible spectral analysis of AgNPs

The absorbance of synthesised biogenic AgNPs was scanned using a UV–visible spectrophotometer (UV-2500 Shimadzu, Japan) at all wavelengths between 200 and 800 nm.

2.4.2. Fourier-transform infrared (FTIR) analysis of AgNPs

The chitosan functional group responsible for the reduction of silver iron and stabilisation of synthesised AgNPs was determined using FTIR (Fourier-transform infrared) spectrometry (FTIR-8400S, Shimadzu, Japan) between 400 and 4000 cm^{-1} at a resolution of 4 cm^{-1}.

2.4.3. Energy-dispersive X-ray spectroscopy (EDX) analysis of AgNPs

The characterisation of elements or chemicals present in the synthesised biogenic AgNPs was determined using energy-dispersive X-ray spectroscopy (EDX-8100, Shimadzu, Japan).

2.4.4. Scanning electron microscopy (SEM) examination of AgNPs

Morphological features of the synthesised biogenic AgNPs were analysed using FE-SEM (field emission scanning electron microscopy, Zeiss SUPRA 55-VP, Cambridge CB1, UK).

2.4.5. Transmission electron microscope (TEM) examination of AgNPs

The size and shape of the synthesised biogenic AgNPs were examined using a transmission electron microscope (100 kV TEM; Morgagni 268, Philips–FEI, Hillsboro, Oregon, USA).

2.4.6. X-ray diffractometer (XRD) pattern analysis of AgNPs

The crystal structure, phase and texture of the synthesised biogenic AgNPs were analysed using an X'Pert Pro X-ray diffractometer (PANalytical BV; Almelo, The Netherlands) operating at a voltage of 40 kV, a running current of 30 mA with Cu Kα radiation.

2.5. In vitro anticancer efficacy of AgNPs

2.5.1. Cell culture and chemicals

Human hepatocellular carcinoma HepG2 cells were purchased from the National Centre for Cell Sciences (NCCS), Pune, India. The cells were maintained in Dulbecco's modified eagle's medium (DMEM) supplemented with 2 mM L-glutamine and balanced salt solution (BSS) adjusted to contain 1.5 g/L Na_2CO_3, 0.1 mM nonessential amino acids, 1 mM sodium pyruvate, 2 mM L-glutamine, 1.5 g/L glucose, 10 mM (4-(2-hydroxyethyl)-1-piperazineethane sulfonic acid) (HEPES) and 10% fetal bovine serum (Gibco, USA). Penicillin and streptomycin (100 IU/100 μg) were adjusted to concentrations of 1 mL/L. The cells were maintained at 37 °C and 5% CO_2 in a humidified CO_2 incubator.

2.5.2. Cytotoxicity assay

The inhibitory concentration (IC_{50}) of the synthesised AgNPs was determined using the MTT [3-(4,5-dimethylthiazol-2-yl)-2,5-diphenyltetrazolium bromide] assay. Briefly, HepG2 cells were grown in a 96-well plate at a density of 1×10^6 cells/well for 48 h. The media was replaced with fresh media containing serially diluted synthesised AgNPs (20–100 μg/ml), and the cells were incubated an additional 48 h. The culture medium was removed, and 100 μL of freshly prepared MTT (Hi-Media, LBS marg, Mumbai, India) solution was added to each well and the plates were incubated at 37 °C for 4 h. After removal of the supernatant, 50 μL of DMSO was added to each of the wells and incubated for 10 min to solubilise the formazan crystals. Doxorubicin (Dox) was used as a standard. The optical density was measured at 620 nm in an ELISA multi-well plate reader (Thermo Multiskan EX, Fisher, USA). The OD was used to calculate the percentage of viable cells:

$$\%\text{viability} = \text{OD of experimental sample}/\text{OD of experimental control} \times 100.$$

2.5.3. Trypan blue dye exclusion assay

The efficacy of the synthesised AgNPs on cell cytotoxicity (percentage quantification) was determined using the trypan blue exclusion assay (Sigma Aldrich, Saint Louis, MO 63103, USA). Briefly, HepG2 cells were grown in a 6-well plate at a density of 3×10^6 cells/well for 24 h. The medium was replaced with fresh medium containing serially diluted synthesised AgNPs (25, 50 and 75 μg/ml), and the cells were incubated for an additional 12 h. The culture medium was removed and 100 μL of the trypan blue (HiMedia) dye was added to each well and visualised by microscopy.

2.5.4. DNA fragmentation assay

The mode of cell death was determined using the DNA fragmentation laddering assay. Briefly, the cells (3×10^6) were treated with synthesised AgNPs at various (25, 50 and 75 μg/ml) concentrations and incubated for 12 h. Then the cells were independently suspended in 10 ml of buffer containing 10 mM Tris HCl and 10 mM EDTA (pH 8.0). Cells were then treated with 10 ml of a solution containing 10 mM Tris HCl, 10 mM EDTA (pH 8.0), 2% SDS and 20 mg/ml proteinase K. The mixture was incubated at 37 °C for 3 h, followed by DNA extraction with phenol: chloroform: isoamyl alcohol solution (in the ratio 25:24:1). The DNA was treated with RNase at a concentration of 20 mg/ml at 4 °C for 45 min and precipitated with 100 ml of 2.5 M sodium acetate and ethanol (DNA solution to ethanol ratio of 1:3). The

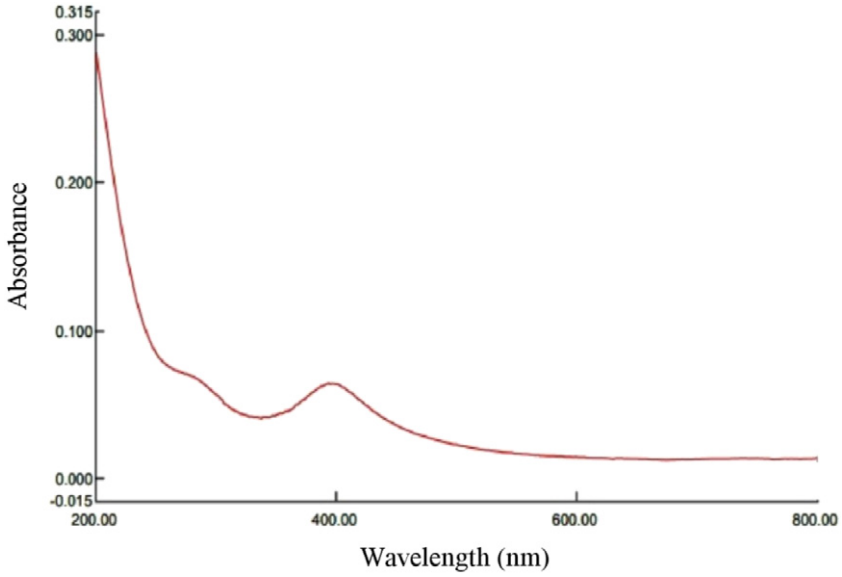

Fig. 1. UV–visible absorption spectrum of the chitosan-synthesised AgNPs.

DNA fragmentation was analysed by electrophoresis for 1 h at 20 V on 2% agarose gel containing ethidium bromide and including 100 base pair marker DNA. The DNA fragment was investigated using a UV-luminated camera.

2.5.5. Western blot analysis

After the experimental period, the cells were lysed with lysis buffer (0.1 ml of lysis buffer for each plate) for 20 min. The supernatants were collected by centrifugation at 10,000 ×*g* for 5 min at 4 °C and were used as cell protein extracts. The harvested protein concentration was measured using a protein assay kit (Bio-Rad, California, USA). The same amount of protein from each extract was used for 10% SDS-polyacrylamide gel electrophoresis. Proteins were transferred onto a nitrocellulose membrane (Millipore, Bangalore, India) and then blocked for 1 h using 10% skim milk. After washing 3× in PBS containing 0.1% Tween, primary antibodies against caspase-3, caspase-9 and beta-actin

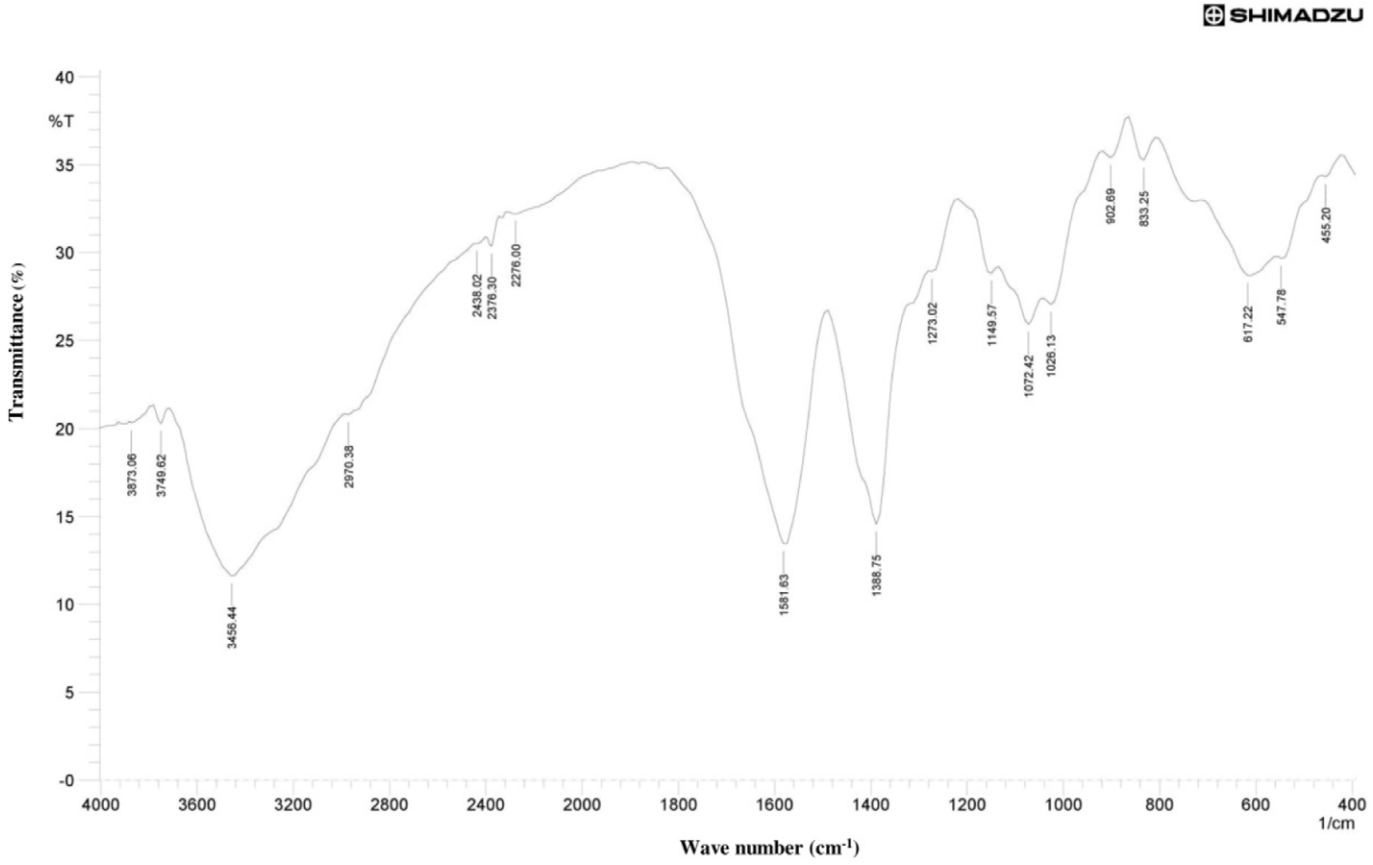

Fig. 2. FTIR spectrum of the chitosan-synthesised AgNPs.

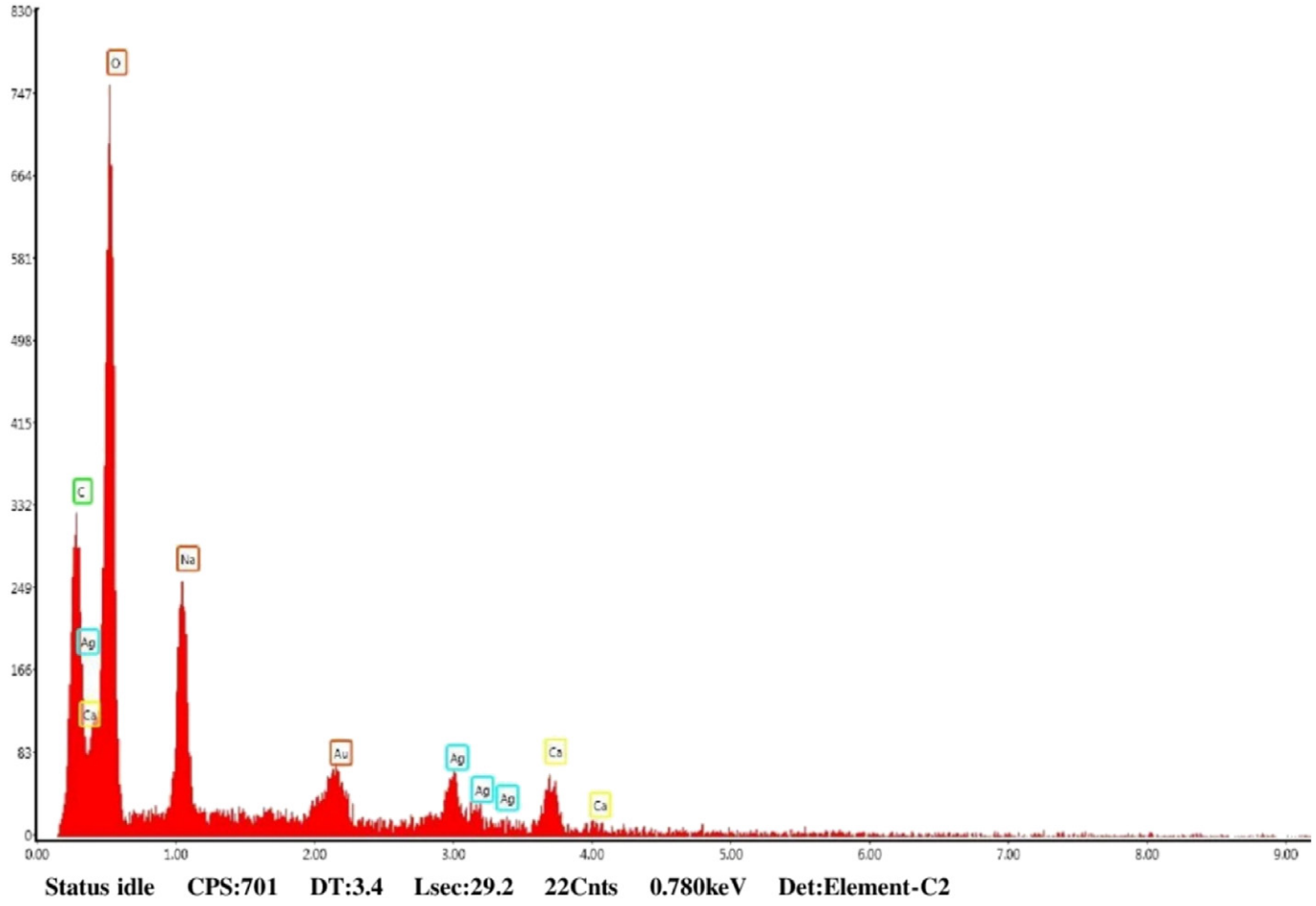

Fig. 3. EDX spectrum revealing peak between 0 and 4 keV, confirming the presence of silver.

(housekeeping control) were added at a v/v ratio of 1:1000. After incubating overnight at 4 °C, the primary antibodies were washed away and secondary antibodies were added and incubated for 1 h at room temperature. The blot was then incubated with chemiluminescence substrate and band visualisation was achieved using an enhanced chemiluminescence kit, and a photo of results was taken.

2.5.6. Statistical analysis

The data were analysed using an ANOVA test, followed by *t*-test using the software Statistician. Values were expressed as the mean with the standard error of the mean; significance level was considered at least with $p < 0.05$.

3. Results and discussion

3.1. Characterisation of AgNPs

Biologically synthesised AgNPs have applied in many fields such as biomolecular detection, diagnostics, antimicrobial studies, therapeutics, catalysis and microelectronics. Particularly in therapeutics, AgNPs have a tremendous number of applications including cancer treatment, skin ointments and creams containing silver to prevent burn and open wound infection, and preparation of medical devices and implants [15,16]. Many nanoparticles have been synthesised using microorganisms, plants and their by-products. In the last few decades, AgNP synthesis strategies have received increasing interest in a search for commercially cost-effective and eco-friendly synthesis routes [17]. In this study, we reported on the synthesis of AgNPs using chitosan extracted from shrimp shell and functionally characterised those AgNPs using an *in vitro* anti-cancer assay.

3.1.1. UV–visible spectrometry analysis

The formation of biogenic AgNPs was confirmed using UV–visible spectrometry from 200 to 800 nm. The surface plasmon resonance (SPR) pattern of the AgNPs synthesised using chitosan showed a distinct absorption peak at 400 nm (Fig. 1). The solution colour changing from creamy white to light yellow and finally to yellowish-brown was observed visually and this also confirmed the formation of AgNPs. The colour intensity light changed from light to dark brown due to the SPR of the AgNPs, and the SPR of the synthesised AgNPs revealing a typical absorption peak at 400 nm provided additional confirmation of the presence of AgNPs. The results of the present study were consistent with another report that determined the optical absorption spectra of the AgNPs are mainly controlled by SPR and the absorption peak correlated with particle size. [18]

3.1.2. FTIR spectrum analysis

FTIR spectrum analysis revealed the functional group of chitosan responsible for the bio-reduction of the silver ion and stabilisation of synthesised AgNPs. The FTIR profile of the chitosan extract (Fig. 2) revealed 18 peaks at 3873, 3749, 3456, 2970, 2438, 2376, 2276, 1581, 1388, 1273, 1149, 1072, 1026, 902, 833, 617, 547 and 455 cm^{-1}. The significant peaks were at 3456 cm^{-1} (corresponding to OH groups), 2970 cm^{-1} (NH stretching group), 2438 cm^{-1} (CH stretching group), 1581 cm^{-1} (NH cutting and bending), 1388 cm^{-1} (deformation vibration mode of CH_3), 1072 cm^{-1} (C-O-C group stretching in protein), 902 cm^{-1} (NH_2 group) and 617 cm^{-1} (NH group). The presence of these particular

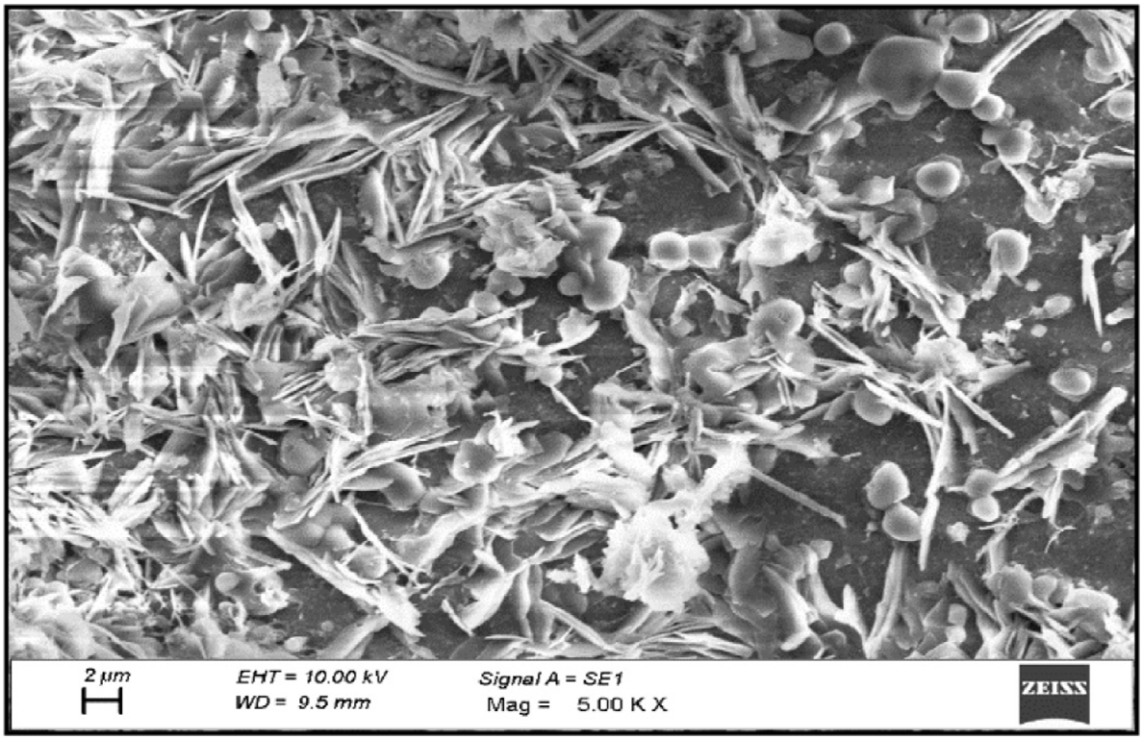

Fig. 4. Scanning electron microscopy image of the biosynthesised AgNPs.

peaks strongly supports the idea that chitosan exhibited capping on the synthesised AgNPs to stabilise them. Our study results agree with those of another study that reported that the biological components interact with metal salts and mediate the reduction process with their functional groups [19]. FTIR analysis, in identifying the functional group of chitosan biomass responsible for the bio-reduction of silver iron and stabilisation of synthesised AgNPs, demonstrated the relationship between the enzyme and substrate during the catalytic process.

3.1.3. EDX analysis of AgNPs

The EDX spectrum, used to characterise all elements or chemicals present in the synthesised AgNPs, revealed a peak from 0 to 4 keV, confirming the presence of silver (Fig. 3). The spectrum at 0.3 and 3 keV shows an intensive signal for silver (representing AgNPs) and corresponding to a 21% atomic percentage of silver. In addition, EDX spectra confirmed a high atomic weight percentage of oxygen and carbon, possibly due to emission from proteins [20]. EDX spectra peaks revealed numerous additional elements, including Ca, Na and Au [21].

3.1.4. SEM examination of AgNPs

The SEM image showed that the synthesised AgNPs were spherical and the particles were polydispersed and non-agglomerated (Fig. 4), the latter of which may be due to control of physical AgNP dehydration during the SEM analysis sample preparation methodology [22].

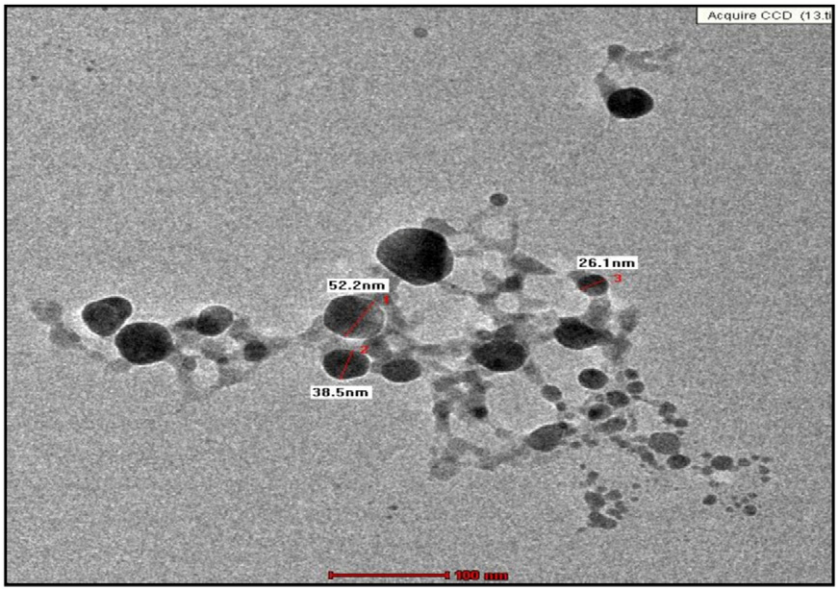

Fig. 5. Transmission electron microscopy image of the bio-produced AgNPs.

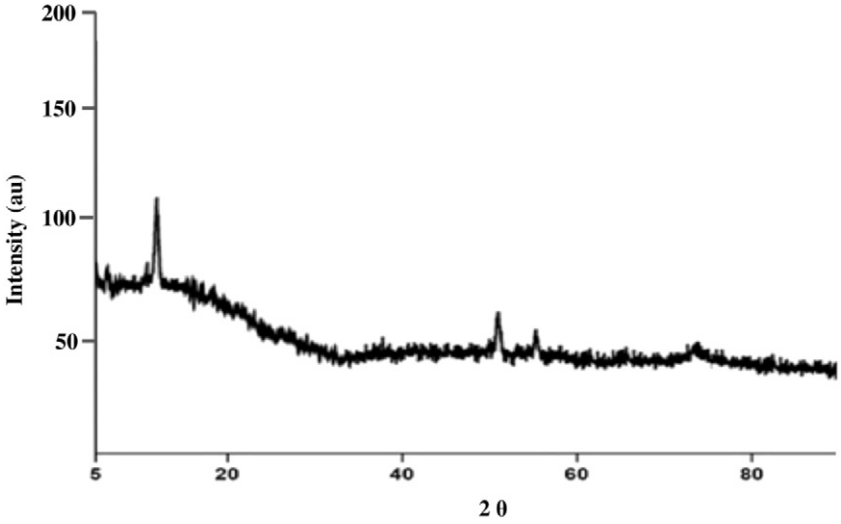

Fig. 6. X-ray diffraction pattern of biosynthesised AgNPs.

3.1.5. TEM examination of AgNPs

TEM is the most important technique to visualise the morphology and particle size distribution of nanoparticles. TEM images revealed that the synthesised AgNPs were spherical with most particles 17–50 nm (Fig. 5), while very few particles were above wavelength. Our study results agreed with those previously reported in a study of biological compounds used as reducing and stabilising agents [23].

3.1.6. XRD pattern analysis of AgNPs

The crystalline structure and size of the AgNPs were investigated by XRD. The XRD pattern of the AgNPs (Bragg's reflections at 2θ between 30 and 80°) detected four diffraction signals at 49°, 59° and 74°, corresponding to (220), (221) and (222). This indicates that the AgNPs had a spherical structure and were crystalline. The sharp peak showed the presence of another biological compound in the synthesised NPs [24]. The peak pattern indicated the reflection planes confined the presence of the spherical shape of Ag and no crystalline impurity peak was observed [25,26] (Fig. 6).

3.2. In vitro anticancer activity of AgNPs

3.2.1. MTT assay

The cytotoxic effect of AgNPs was determined against HepG2 cells exposed to 20–100 μg/ml in the MTT assay. The cell viability rate of HepG2 cells is represented in Fig. 7, showing an increase with increasing concentration of chitosan-mediated AgNPs. The amount of AgNPs required to decrease the viability of HepG2 cells to 50% of the initial population (IC_{50}) was 48 ± 1.0 μg/ml and the doxorubicin (standard) required to decrease the viability of HepG2 cells to 50% of the initial population was 16 ± 1.0 μg/ml. Hepatocellular carcinoma is the predominant primary liver cancer and it is the fifth most common cancer in the world [27]. However, current conventional treatments are not effective in managing hepatocellular carcinoma patients. Therefore, researchers have investigated new and effective approaches for the management of hepatocellular carcinoma with minimal side effects. Recently, many researchers have reported that AgNPs possess therapeutic cancer treatment potential because of their unique properties. In this study, biogenic AgNPs induced intracellular oxidative stress in HepG2 cells, and AgNPs agglomerated in the cytoplasm and nuclei of the treated cells. The results showed dose-

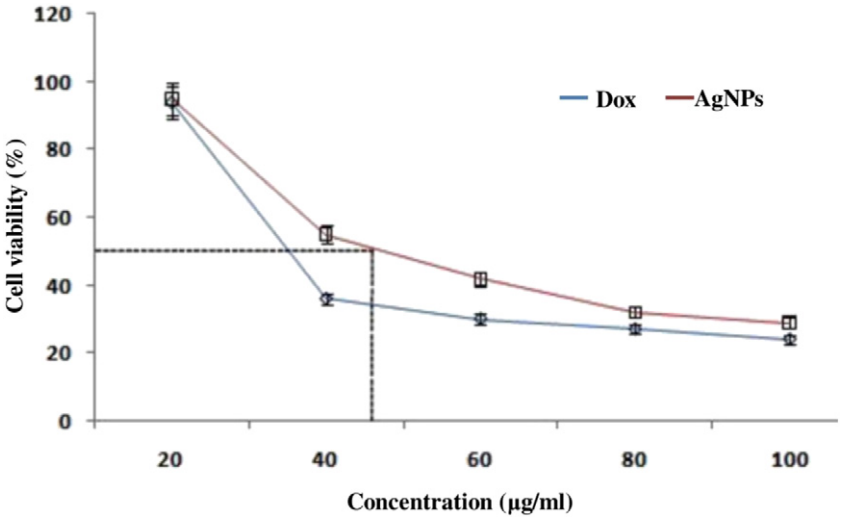

Fig. 7. Dose-dependent cytotoxicity effect of biosynthesised AgNPs on the proliferation of human hepatocellular carcinoma HepG2 cells by MTT assay.

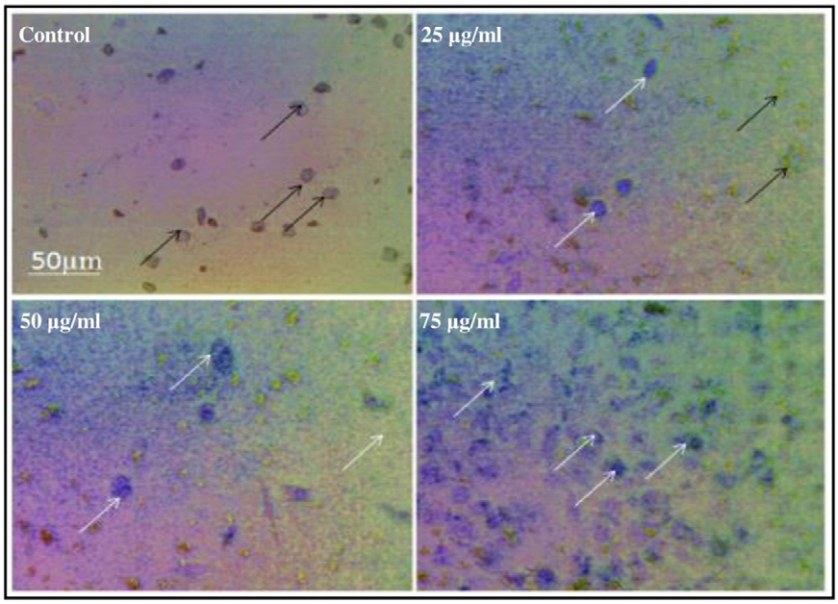

Fig. 8. Dose-dependent cell viability effects of biosynthesised AgNPs on human hepatocellular carcinoma HepG2 cells by the trypan blue exclusion assay.

dependent cytotoxicity of HepG2 cells after 24 h of AgNPs treatment. The study revealed a relatively low concentration of AgNPs rapidly decreased HepG2 cell viability. Therefore, we selected 25, 50 and 75 µg/ml concentration of synthesised AgNPs for further apoptotic experiment. Several studies have reported that green-synthesised AgNPs, using many extracts, demonstrated remarkable anticancer properties [28]. Also, AgNPs have been shown to induce cytotoxicity by induction of oxidative stress [29].

3.2.2. Trypan blue exclusion assay

The trypan blue exclusion image revealed the cytotoxic efficacy of the synthesised AgNPs in a dose-dependent manner, with viable cells appearing colourless, and the non-viable cells blue (Fig. 8). The IC_{50} value of AgNPs against HepG2 cells, determined in the MTT assay, resulted in inhibited growth of HepG2 cells in concentrations similar to those from previous reports [30,31]. These results should encourage further analysis of the anticancer activity of AgNPs on HepG2 cells.

3.2.3. DNA fragmentation analysis

Apoptosis was induced to compare the DNA ladder fragmentation pattern with the products of endonuclease cleavage in apoptosis. The DNA of HepG2 cells was treated with various concentrations of AgNPs (25, 50 and 75 µg/ml) and electrophoresed on agarose gel. The results are shown in Fig. 9. In the AgNP-treated cells, the interaction between AgNPs and cellular components resulted in DNA damage and cell death. Interestingly, HepG2 cells treated with AgNPs revealed that the number of cells that experienced apoptosis increased with increasing concentrations of AgNPs. The current results were in agreement with a similar report detailing the cytotoxic effect of mulberry on HepG2 cells due to the introduction of AgNPs [32].

3.2.4. Western blot

The synthesised AgNPs upregulated the caspase 3 and 9 protein expression levels compared to the control cells (Fig. 10). Apoptosis is a natural mechanism of programmed cell death which can be activated by a variety of intra- and extracellular factors. AgNPs induce cytomorphological changes on HepG2 cells in terms through oxidative stress, cell shrinkage and biochemical reactions, resulting in apoptosis [33]. AgNPs can induce the lipid degradation that results in DNA deterioration, necrosis and apoptosis [34]. Pro- and anti-apoptotic proteins play a key role in tumour expansion and progression [38], so apoptosis is considered an important pathway in cancer treatment. Our results revealed that the executor caspase 3 and initiator caspase 9 were significantly upregulated in HepG2 cells treated with AgNPs synthesised from chitosan compared to control cells. Other recent reports have demonstrated apoptotic cell death due to the introduction of AgNPs [35], including biologically synthesised AgNPs [36]. The biogenic AgNPs synthesised from chitosan effectively induced apoptosis by regulating the intrinsic pathway. Therefore, synthesised AgNPs can be an effective molecule for cancer therapy. Regardless of the favourable benefits of AgNPs, safety concerns have been voiced globally on the use of AgNPs due to their cytotoxicity in living organisms. This study presented multiple *in vitro* models that revealed the ability of AgNPs to

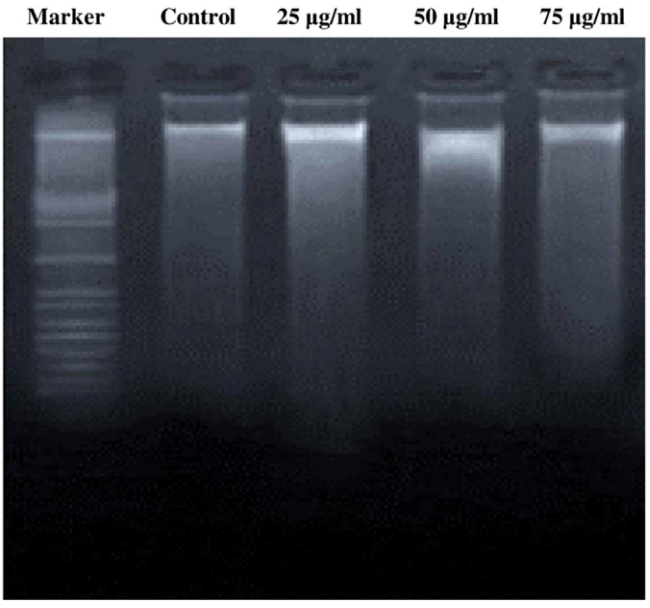

Fig. 9. Dose-dependent apoptotic effects of biosynthesised AgNPs on human hepatocellular carcinoma HepG2 cells by DNA laddering.

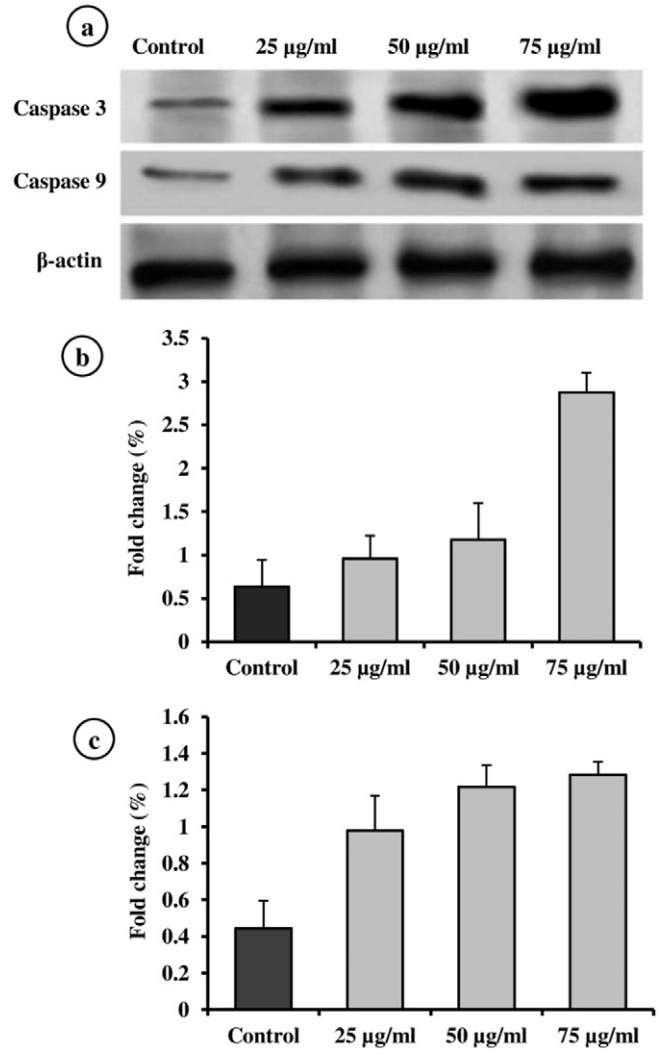

Fig. 10. (a) Western blot determination of proteins caspase 3 and caspase 9 relative to β-actin against HepG2 cells exposed to biosynthesised AgNPs for 12 h. (b) revealed the quantification of caspase 3 immunoblot by densitometry and (c) revealed the quantification of caspase 9 immunoblot by densitometry.

induce cytotoxicity by increased oxidative stress, DNA fragmentation, apoptosis and inflammation [37].

4. Conclusion

For the first time, chitosan extracted from shrimp shells was successfully used as a reducing agent to synthesise biogenic AgNPs *via* an eco-friendly, green approach and those AgNPs demonstrated anticancer activity against human carcinoma HepG2 cells. The optimum precursor concentration and time to synthesise AgNPs were found to be 1% and 12 h, respectively. The formation of AgNPs was characterised by UV–vis, the functional group was characterised by FTIR, presence of elements determined by EDX, surface morphology was characterised by SEM, shape and particle-sized was analysed by TEM, and the crystalline structure was investigated by XRD. Study results proved that the biosynthesised AgNPs possessed cytotoxicity and apoptotic potential against human hepatocellular carcinoma HepG2 cells, and could play an important role in pharmaceutical, medicinal and therapeutic applications. However promising the advantages of AgNPs, safety concerns have been raised on the use of AgNPs because of their bioaccumulation and toxic effects in living organisms. More studies are needed to evaluate the bioaccumulation and toxicity of AgNPs.

CRediT authorship contribution statement

Kannappan Priya: Conceptualization, Methodology, Software, Visualization, Investigation, Supervision, Writing - review & editing. **Mayakrishnan Vijayakumar:** Data curation, Writing - original draft, Visualization, Investigation, Software, Validation, Writing - review & editing. **Balakarthikeyan Janani:** Visualization, Investigation.

Declaration of competing interest

No competing interests between all authors.

Acknowledgements

We are grateful to the University Grants Commission (Project title: Antiproliferative activity of silver complexed chitosan nanocomposites isolated from shrimp shell against HepG2 cells; Project No: MRP-6353/16 (SERO/UGC)), New Delhi, India for their financial assistance.

References

[1] L. Filipponi, D. Sutherland, Introduction to Nanoscience and Nanotechnologies, NANOYOU Teachers Training Kit in Nanoscience and Nanotechnologies, Aarhus University, Denmark, 2010 1–29.
[2] K.N. Thakkar, S.S. Mhatre, R.Y. Parikh, Biological synthesis of metallic nanoparticles, Nanomedicine: Nanotechnol. Biol. Med. 6 (2010) 257–262.
[3] S. Nagarajan, K. Arumugam Kuppusamy, Extracellular synthesis of zinc oxide nanoparticle using seaweeds of gulf of Mannar, India, J. Nanobiotechnol. 11 (2013) 1–11.
[4] C.K.S. Rajeshkumar, G. Annadurai, Green synthesis of silver nanoparticles using marine brown algae *Turbinaria conoides* and its antibacterial activity, Int. J. Pharma Biosci. 3 (2012) 502–510.
[5] K.M.M.A. El-Nour, A. Eftaiha, A. Al-Warthan, R.A.A. Ammar, Synthesis and applications of silver nanoparticles, Arab. J. Chem. 3 (2010) 135–140.
[6] N. Faisal, K. Kumar, Polymer and metal nanocomposites in biomedical applications, Bioint. Res. Appl. Chem. 7 (2017) 2286–2294.
[7] M. AL-Katib, Y. AL-Shahri, A. AL-Niemi, Biosynthesis of silver nanoparticles by cyanobacterium *Gloeocapsa* sp, Int. J. Enhan. Res. Sci. Technol. Eng. 4 (2015) 2319–7463.
[8] P. Mohanpuria, N.K. Rana, S.K. Yadav, Biosynthesis of nanoparticles: technological concepts and future applications, J. Nanopart. Res. 10 (2008) 507–517.
[9] J. Huang, Q. Li, D. Sun, Y. Lu, Y. Su, X. Yang, H. Wang, Y. Wang, W. Shao, N. He, Biosynthesis of silver and gold nanoparticles by novel sundried *Cinnamomum camphora* leaf, Nanotechnol 18 (2007) 1–11.
[10] A.K. Shukla, S. Iravani, Metallic nanoparticles: green synthesis and spectroscopic characterization, Environ. Chem. Lett. 15 (2017) 223–231.
[11] S. Zhang, L. Yin, J. Wang, W. Zhang, L. Zhang, X. Zhu, A green platform for preparation of the well-defined polyacrylonitrile: 60Co γ-ray irradiation-initiated RAFT polymerization at room temperature, Polymers 9 (2017) 26–36.
[12] L.S. Wang, C.Y. Wang, C.H. Yang, C.L. Hsieh, S.Y. Chen, C.Y. Shen, J.J. Wang, K.S. Huang, Synthesis and anti-fungal effect of silver nanoparticles–chitosan composite particles, Int. J. Nanomedicine 10 (2015) 2685–2696.
[13] M.M. Islam, S.M. Masum, M.M. Rahman, M.A. Islam Molla, A.A. Shaikh, S.K. Roy, Preparation of chitosan from shrimp shell and investigation of its properties, Int. J. Basic App. Sci. 11 (2011) 77–80.
[14] P. Sanpui, A. Chattopadhyay, S.S. Ghosh, Induction of apoptosis in cancer cells at low silver nanoparticle concentrations using chitosan nanocarrier, ACS Appl Mater Interf 3 (2011) 218–228.
[15] S. Balasubramanian, U. Jeyapaul, S.M.J. Kala, Antibacterial activity of silver nanoparticles using *Jasminum auriculatum* stem extract, Int. J. Nanosci. 18 (2017) 1850011.
[16] R. Vijayan, S. Joseph, B. Mathew, Anticancer, antimicrobial, antioxidant, and catalytic activities of green synthesized silver and gold nanoparticles using *Bauhinia purpurea* leaf extract, Bioprocess Biosyst. Eng. 42 (2019) 305–319.
[17] B. Senthil, T. Devasena, B. Prakash, A. Rajasekar, Non-cytotoxic effect of green synthesized silver nanoparticles and its antibacterial activity, J. Photochem. Photobiol. B Biol. 177 (2017) 1–7.
[18] R. Kalaivani, M. Maruthupandy, T. Muneeswaran, A. Hameedha Beevi, M. Anand, C.M. Ramakritinan, A.K. Kumaraguru, Synthesis of chitosan mediated silver nanoparticles (Ag NPs) for potential antimicrobial applications, Front. Lab. Med. 2 (2018) 30–35.
[19] A. Ajitha, Y.A.K. Reddy, P.S. Reddy, Biogenic nano-scale silver particles by *Tephrosia purpurea* leaf extract and their inborn antimicrobial activity, Spectrochim. Acta Mol. Biomol. Spectrosc. 121 (2014) 164–172.
[20] P. Mukherjee, A. Ahmad, D. Mandal, S. Senapati, S.R. Sainkar, M.I. Khan, R. Parishcha, P.V. Ajaykumar, M. Alam, R. Kumar, M. Sastri, Fungus-mediated synthesis of silver nanoparticles and their immobilization in the mycelial matrix: a novel biological approach to nanoparticle synthesis, Nano Lett. 1 (2001) 515–519.
[21] T. Tarko, A. Duda-Chodak, M. Kobus, Influence of growth medium composition on synthesis of bioactive compounds and antioxidant properties of selected strains of *Arthrospira* cyanobacteria, Czech J. Food Sci. 30 (2012) 258–267.

[22] M. Sigamoney, S. Shaik, P. Govender, S.B.N. Krishna, Sershen, African leafy vegetables as bio-factories for silver nanoparticles: a case study on *Amaranthus dubius* C Mart. Ex Thell, South Afr, J. Bot 103 (2016) 230–240.
[23] S.M. Ghaseminezhad, S. Hamedi, S.A. Shojaosadti, Green synthesis of silver nanoparticles by a novel method: comparative study of their properties, Carbohyd. Polym. 89 (2012) 467–472.
[24] S.S. Shankar, A. Rai, A. Ahmad, M. Sastry, Rapid synthesis of Au, Ag, and bimetallic Au core-Ag shell nanoparticles using Neem (*Azadirachta indica*) leaf broth, J. Coll. Inter. Sci. 275 (2004) 496–502.
[25] K.A. Bogle, S.D. Dhole, V.N. Bhoraskar, Silver nanoparticles: synthesis and size control by electron irradiation, Nanotechnol 17 (2006) 3204.
[26] R. Zamiri, A. Zakaria, M.S. Husin, Z.A. Wahab, F.K. Nazarpour, Formation of silver microbelt structures by laser irradiation of silver nanoparticles in ethanol, Int. J. Nanomedicine 6 (2011) 2221–2224.
[27] S.V. Nair, M. Hettihewa, H. Rupasinghe, Apoptotic and inhibitory effects on cell proliferation of hepatocellular carcinoma HepG2 cells by methanol leaf extract of *Costus speciosus*, Biomed. Res. Int. 2014 (2014) 1–10.
[28] S. Kummara, M.B. Patil, T. Uriah, Synthesis, characterization, biocompatible and anticancer activity of green and chemically synthesized silver nanoparticles – a comparative study, Biomed. Pharmacother. 84 (2016) 10–21.
[29] S. Kim, J.E. Choi, J. Choi, K.H. Chung, K. Park, J. Yi, D.Y. Ryu, Oxidative stress-dependent toxicity of silver nanoparticles in human hepatoma cells, Toxicol. in Vitro 23 (2009) 1076–1084.
[30] M. Yousefi, S.H. Ghaffari, A. Zekri, S. Hassani, K. Alimoghaddam, A. Ghavamzadeh, Silibinin induces apoptosis and inhibits proliferation of estrogen receptor (ER)-negative breast carcinoma cells through suppression of nuclear factor kappa B activation, Arch. Iran. Med. 17 (2014) 366–371.
[31] Y. Ge, Y. Zhang, Y. Chen, Q. Li, J. Chen, Y. Dong, W. Shi, Silibinin causes apoptosis and cell cycle arrest in some human pancreatic cancer cells, Int. J. Mol. Sci. 12 (2011) 4861–4871.
[32] S.A. Fathy, A.N.B. Singab, S.A. Agwa, D.M.A. El Hamid, F.A. Zahra, S.M.A. El Moneim, The antiproliferative effect of mulberry (*Morus alba* L.) plant on hepatocarcinoma cell line HepG2, Egypt. J. Med. Human Gen. 14 (2013) 375–382.
[33] F.M. Jannathul, P. Lalitha, Apoptotic efficacy of biogenic silver nanoparticles on human breast cancer MCF-7 cell lines, Prog. Biomater. 4 (2015) 113–121.
[34] T. Xia, M. Kovochich, J. Brant, M. Hotze, J. Sempf, T. Oberley, C. Sioutas, J.I. Yeh, M.R. Wiesner, A.E. Nel, Comparison of the abilities of ambient and manufactured nanoparticles to induce cellular toxicity according to an oxidative stress paradigm, Nano Lett. 6 (2006) 1794–1807.
[35] Y. Pan, S. Neuss, A. Leifert, M. Fischler, F. Wen, U. Simon, G. Schmid, W. Brandau, W. Jahnen-Dechent, Size-dependent cytotoxicity of gold nanoparticles, Small 3 (2007) 1941–1949.
[36] A. Stroh, C. Zimmer, C. Gutzeit, M. Jakstadt, F. Marschinke, T. Jung, H. Pilgrimm, T. Grune, Iron oxide particles for molecular magnetic resonance imaging cause transient oxidative stress in rat macrophages, Free Rad. Biol. Med. 36 (2004) 976–984.
[37] B.H. Mao, Z.Y. Chen, Y.J. Wang, S.J. Yan, Silver nanoparticles have lethal and sub lethal adverse effects on development and longevity by inducing ROS-mediated stress responses, Sci. Rep. 8 (2018) 1–16.
[38] S. Gunaseelan, A. Balupillai, K. Govindasamy, K. Ramasamy, G. Muthusamy, M. Shanugan, et al., Linalool prevents oxidative stress activated protein kinases in single UVB-exposed human skin, PLos ONE 8 (5) (2017), e0176699.